TIP CLEARANCE HEAT TRANSFER AND DESENSITIZATION IN HIGH PRESSURE TURBINES

Michael Durham, Jay Kapat, Alain Kassab and Joseph Tapley
Department of Mechanical, Materials & Aerospace Engineering
University of Central Florida
Orlando, FL 32816-2450

Charles MacArthur and Douglas Rabe
Air Force Research Laboratory, AFRL-PRT
WPAFB, OH 45433-7251

Abstract

This paper reports the partial progress made so far for this new project, which started in August 1999. The focus of this project is tip heat transfer, which is one of the key factors responsible for limiting the life of a gas turbine blade. The project will involve rotating experiments under representative operating conditions where overall blade efficiency as well as detailed heat transfer and pressure field will be measured.

Rotating experiments will be performed for two cases: no desensitization and tip blowing for clearance desensitization. Two different tip geometries will be tested: flat tip and double squealer tip. Rotating experiments will be performed in a high speed rotating test rig, with one stationary row and one rotating row, in Turbine Research Facility (TRF) of Air Force Research Laboratory (WPAFB, OH). Each row of blades will have about 40 blades, where the actual number will be decided after the blade design is finalized. This project will use high efficiency E^3 (*Energy Efficient Engine*) design, as made available to this project by GE. However, there may be need for modification of this blade design for implementation into the TRF rig as the blade heights are different from what the rig can accommodate.

For each case under investigation, experiments will be performed for different blade loading and corrected speed parameter. A test matrix has been prepared and will be presented in this paper. For each case, blade efficiency is measured by measuring total temperatures and pressures before and after the rotating stage with the help of a rake of probes. Blade and tip surface temperature and pressure distributions will be measured by temperature and pressure sensitive paints, complemented by a few point measurements. A preliminary measurement plan will be presented.

An inverse method, based on BEM (Boundary Element Method) approach, will be used to extract heat transfer coefficients from the measured surface temperature distributions. Some preliminary results about how this methodology works will be presented in this paper. It is found that with the help of appropriate regularization, the method can be used to diminish the sensitivity of the calculated heat transfer coefficients on experimental uncertainty.

A. Overall Objectives

Compare between:
- Different desensitization schemes
- Results obtained here in a high speed facility and
    - CFD prediction
    - Cascade tests
    - Steady, low-speed rotating rig
    - Appropriately scaled engine data

B. Experiments

1. Test Configuration
- Tip configurations (tentative, to be finalized after discussion with collaborators and industrial sponsors)
    - Flat Tip
    - Squealer Tip
    - Flat Tip with Blowing
- Perform tests under at least two different corrected RPMs of the rotor and at least two different initial stage pressure ratios

2. Vane and Rotor Design
- A new turbine vane and rotor set will be fabricated
- E^3 (Energy Efficient Engine) blade design will be used
- This design will be same as the one used in 3-d CFD simulation

3. Test Objectives
At different corrected speeds, as functions of corrected mass flow rates,
- Measure aerodynamic efficiency
- Measure mechanical efficiency
- Document pressure distribution on tip surface and pressure and suction surfaces in the near tip region
- Document temperature distribution on tip surface and pressure and suction surfaces in the near tip region
- Calculate convective heat transfer coefficient for blade tip and near tip region
- Measure inlet and exit "turbulence" intensity
- Identify shock fronts, if any

4. Measurement Plans
- Mass Flow Rate
    - Time history of tank pressure and temperature
- Efficiency
    - Stage inlet and exit total temperatures and pressures
   - Rakes of Kiel probes and thermocouples before and after rotating stage

- Turbulence Intensity
  - Fluctuating velocity time trace
    - Multi-dimensional hot-wire probes
    - Two sets
      - One set upstream, one set down stream
      - Both near tip region and at mid radius
- Surface Pressure and Temperature Distribution
  - TSP and PSP on the tip surface and near tip regions on both pressure and suction sides
- Point Measurements
  - At several locations on tip, pressure, suction and inner shroud surfaces
    - Kulite pressure sensors
    - Thin film gauges for temperature and heat flux

5. Relevant Features of the Facility (Turbine Research Facility, AFRL, WPAFB)

Supply Temperature (with ± 2 *°F* uniformity)	550 *°F*
Supply Pressure	150 *psi*
Test times	1 to 3 *seconds*
Gas (for adjusting specific heat ratio)	$N2 + CO2$
Blade Dimension	
Maximum tip diameter	34 *inches*
Minimum hub diameter	17 *inches*
Speed Control: Maintains the corrected speed	
Maximum physical speed	12000 RPM
Reynolds number, Mach number: Variable	

Some typical numbers

Re = 2 300 000 (vane axial chord, vane exit axial velocity)

M = 0.4 (vane exit condition, stationary frame), M ≈ 1.5 (maximum achievable in rotor frame)
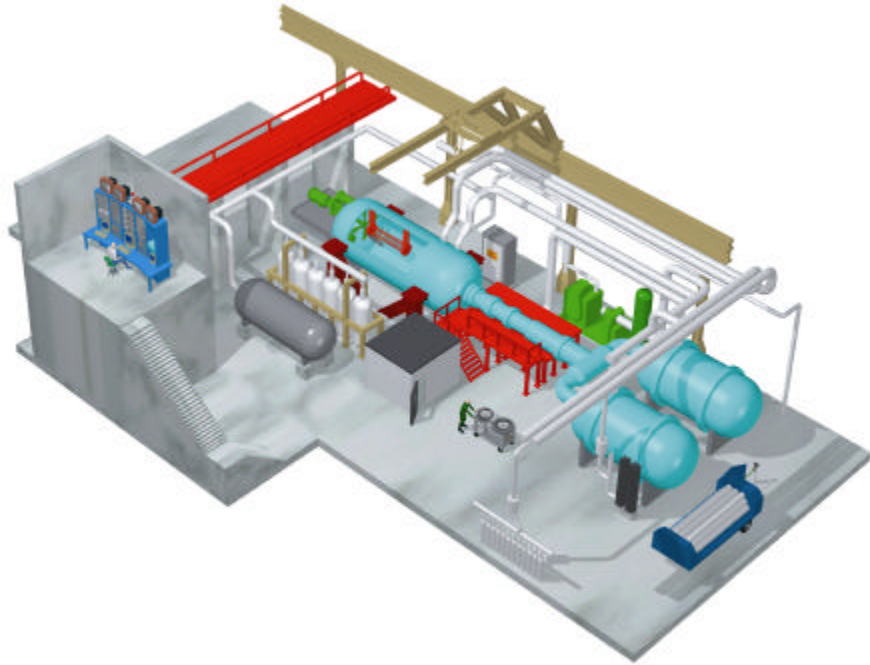
(a) Overall facility
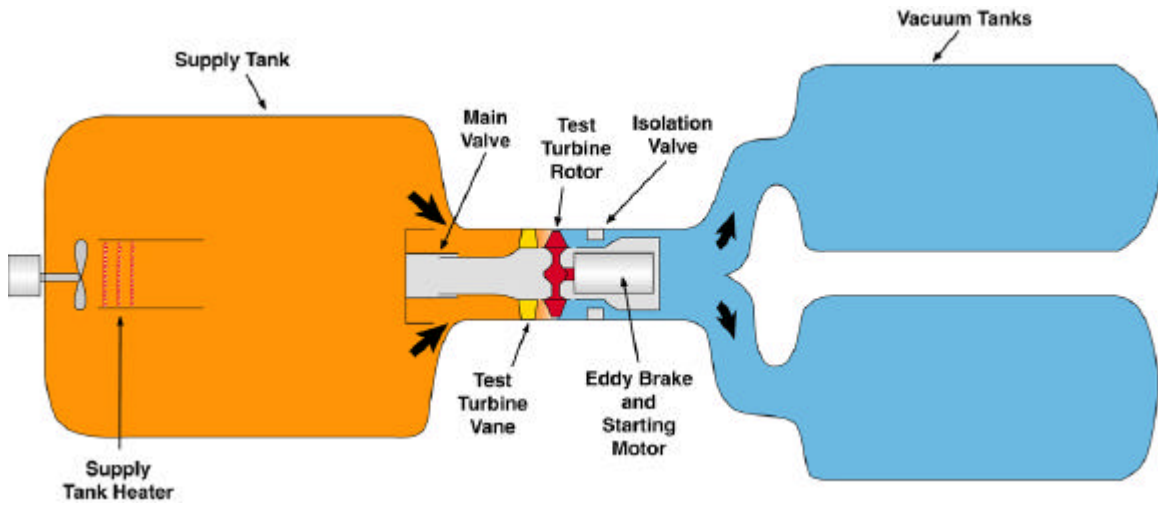

(b) Schematic of test section

Figure 1: Test facility at Air Force Research Laboratory, WPAFB

C. Retrival of Multi-dimensional Heat Transfer Co-efficient Distribution Using An Inverse BEM-based Regularized Algorithm

1. Introduction

- Current practice in heat transfer community to retrieve h:

  $\Rightarrow$ temperature driven physical phenomenon, thermochromic liquid crystals, or thermographic phosphor, to find surface temperature.

  $\Rightarrow$ use 1-D semi-infinite medium solution to compute h

  $$\frac{T_s(t) - T_i}{T_\infty - T_i} = 1 - e^{\left(\frac{h^2 t}{k\rho c}\right)} erfc\left(h\sqrt{\frac{t}{k\rho c}}\right)$$
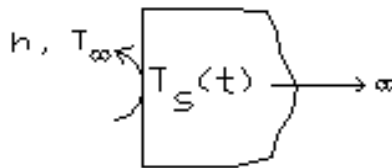
  $\Rightarrow$ measure $T_s(t)$ and solve above for h $\Leftarrow$

- Approach is valid in regions/regimes where heat conduction is 1-D.

- Problems when heat conduction is 2-D or 3-D: corner and step regions, stagnation region of impinging jets, regions downstream of film cooling holes, etc...

- A Solution: boundary element method (BEM) to resolve 2-D and 3-D heat transfer and inverse problem(IP) methods to regularize retrieval of h distributions using surface temperature time history.

- Advantages:

  - BEM -boundary integral equation method requires only surface mesh to solve 2-D or 3-D problem. T or q histories are unknowns at surface nodes.

  - IP- active control of effect of input errors from surface temperature measurement.

2. Methodology

2.1 Boundary Element Method (BEM)

- For diffusion equation, a boundary integral equation (BIE), valid for interior or boundary points, is

$$\rho c\, C(\xi)\, T(\xi, t_F) = \int_{t_0}^{t_F} \oint_{\Gamma} \left[H(x, t, \xi, t_F) T(x, t) - q(x, t) G(x, t, \xi, t_F) \right] d\Gamma dt$$

Γ = domain boundary

ξ = co-ordinates of source point

$H(x, t, \xi, t_F)$ = $-k\, \partial G(x, t, \xi, t_F)/\partial n$

$q(x, t)$ = $-k \frac{\partial T}{\partial n}$

$C(\xi)$ = depends on geometry and location

$G(x, t, \xi, t_F)$ = Green free space (or fundamental) solution

$$G(x, t, \xi, t_F) = \left[\frac{\rho c}{4\pi k(t_F - t)} \right]^{\frac{d}{2}} exp\left[\frac{-\rho c}{4k(t_F - t)} r^2 \right]$$

where $d = 1, 2, 3$ for 1D, 2D, and 3D, and r is the Euclidean distance from field point x to source point ξ

- Discrete form of transient equation

$$[\widehat{H}]^{FF} \{T\}^F - [G]^{FF} \{q\}^F = \underbrace{\sum_{p=1}^{F-1} \left([G]^{Fp} \{q\}^p - [H]^{Fp} \{T\}^p \right)}_{\text{Previous time history convolution}}$$

F — current time level

$\{T\}^F$ — vector of surface nodal temperatures

$\{q\}^F$ — vector of surface nodal heat fluxes

$[H]^{Fp}$, $[G]^{Fp}$ — time dependent influence coefficient matrices

We can subsequently define the right-hand-side vector,

$$\{c\}^F = \underbrace{\sum_{p=1}^{F-1}\left([G]^{Fp}\{q\}^p - [H]^{Fp}\{T\}^p\right)}_{\text{Previous time history convolution}}$$

This equation is solved at every time level F by direct or iterative methods to obtain unknown boundary values. In the steady-state analog, the right-hand-side $\{c\}^F$ is zero and corresponding steady-state influence matrices are used.
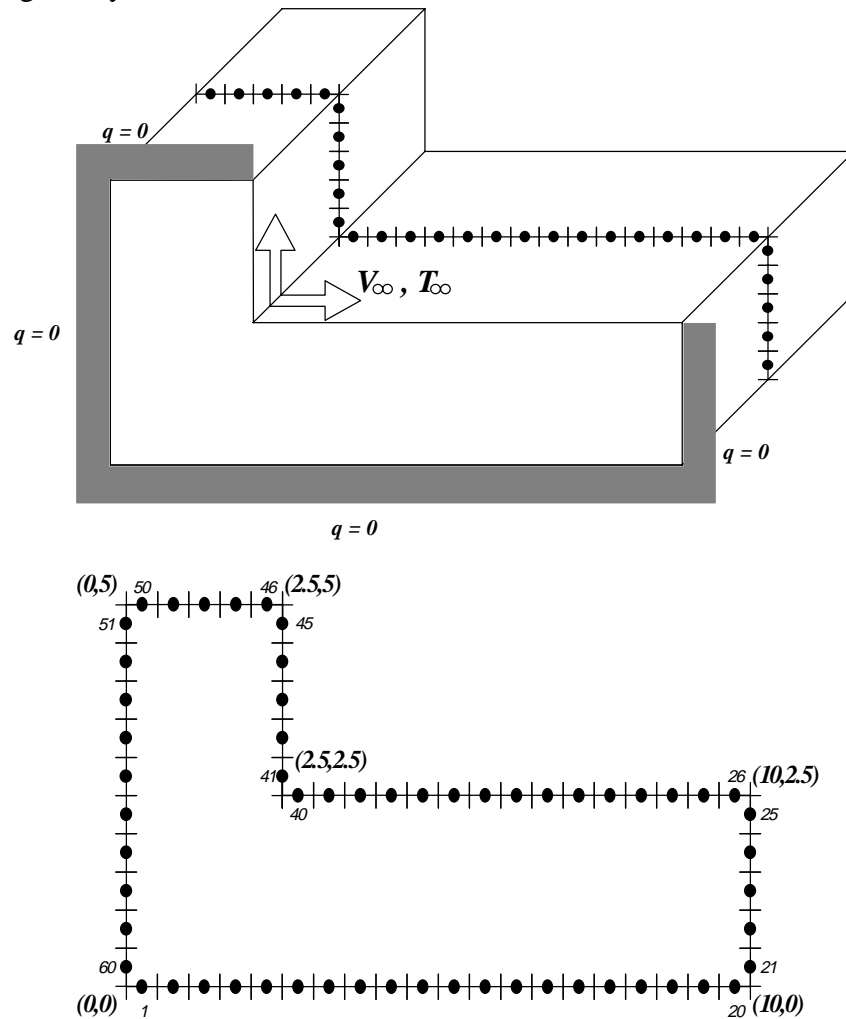

Figure 2: BEM constant element model for a backward-facing step to be considered later in detail in the example section.

2.2 Inverse Problem Formulation

Film coefficient modeling is actually a direct problem due to the fact that time history temperature measurement are imposed as first kind boundary conditions at the convective boundaries. However, small measurement errors at such boundaries result over time into large deviations of computed heat fluxes and consequently erroneous values of h. A remedy for this sensitivity problem is to formulate h retrieval as an inverse problem and to regularize the functional. To this end, the following least-square functional, Z^F, is defined as,

$$Z^F = \sum_{i=1}^{M} \left(\frac{\widehat{T}_i^F - T_i^F}{\Delta T^F} \right)^2 + \beta \sum_{i}^{M} \left(\frac{q_i^F - \overline{q}_i^F}{\Delta q^F} \right)^2$$
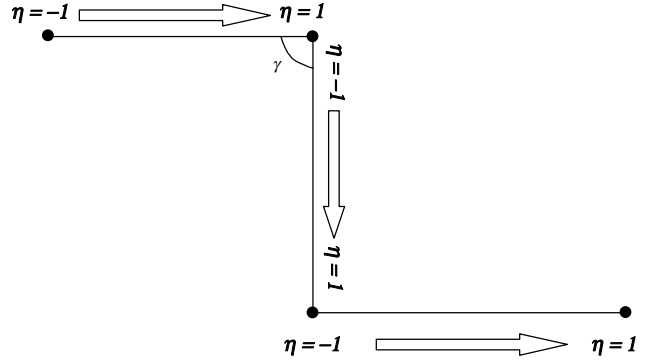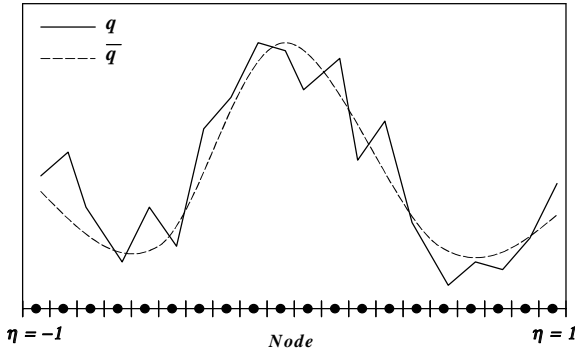
M	number of temperature measuring points at convective boundaries.
$\widehat{T}_i^F$	measured temperatures.
T_i^F	computed temperatures given current estimates of h distribution.
ΔT^F	normalizing temperature difference.
β	regularization (tuning) parameter.
q_i^F	computed fluxes given current estimates of h distribution.
$\overline{q}_i^F$	mean heat flux distribution of currently-computed fluxes.
Δq^F	normalizing heat flux magnitude.

- interpolation is automated if an angle γ is detected between two boundary elements that differs from $180°$ by a fixed amount, say $30°$, a new independent curve-fit is performed.

- The term $\overline{q}\,_i^F$, is obtained by a least-squares fit of current fluxes over the convective boundary evaluated at the measurment points i.

$$\overline{q}\,_i^F = A_{ik}\,q_k^F$$

where A_{ik} is derived from orthogonal polynomial expansion.

- Gram-Schmidt orthogonal polynomials $p_n(x)$ are generated

$$p_{j+1}(\eta) = (\eta - \alpha_{j+1})p_j(\eta) - \beta_j\,p_{j-1}(\eta);\ p_0(\eta) = 1;\ p_{-1}(\eta) = 0$$

where α and β are explicitly given by the expressions,

$$\alpha_{k+1} = \frac{\displaystyle\sum_{i=1}^{M}\eta_i[p_k(\eta_i)]^2}{\displaystyle\sum_{i=1}^{M}[p_k(\eta_i)]^2}\ ,\ \text{and}\quad \beta_k = \frac{\displaystyle\sum_{i=1}^{M}[p_k(\eta_i)]^2}{\displaystyle\sum_{i=1}^{M}[p_{k-1}(\eta_i)]^2}$$

- M is the number of measurment points and η_i's correspond to the boundary nodes along the interpolation path ($-1 < \eta < 1$).

- Keep $P < 5$ to provide smooth $\overline{q}\,(\eta)$ and $P < M$

- Define, $d_{lm} = \displaystyle\sum_{i=1}^{M} p_l(\eta_i)p_m(\eta_i)$, then the interpolated flux is

$$\overline{q}\,_i = p_l(\eta_i)d_{lm}^{-1}p_m(\eta_k)\,q_k$$

Thus

$$A_{ik} = p_l(\eta_i)d_{lm}^{-1}p_m(\eta_k)$$

for i and k corresponding to elements along the current straight path.

- Minimization of functional leads to a linear problem which can be minimized analytically to lead to q equation

- Introduce definition of $\overline{q}\,_i$ into functional and

9

$$Z^F = \frac{1}{(\Delta T^F)^2} \sum_{i=1}^{M} \left(\widehat{T}_i^F - T_i^F \right)^2 + \frac{\beta}{(\Delta q^F)^2} \sum_{i=1}^{M} \left(B_{ik} \, q_k^F \right)^2$$

where the matrix $B_{ik} = \delta_{ik} - A_{ik}$, and δ_{ik} is the Krönecker delta.

- Differentiating with respect to heat fluxes q_j^F at each of the convective nodes and setting to zero,

$$\frac{\partial Z^F}{\partial q_j^F} = \frac{2}{(\Delta T^F)^2} \left(T_i^F - \widehat{T}_i^F \right) \frac{\partial T_i^F}{\partial q_j^F} + \frac{2\beta}{(\Delta q^F)^2} B_{ik} \, q_k^F B_{ik} \delta_{kj} = 0$$

- Defining the sensitivity coefficients
$$X_{ij} = \partial T_i^F / \partial q_j^F$$
then
$$X_{ij} \left(\widehat{T}_i^F - T_i^F \right) = m^F \beta \, C_{jk} \, q_k^F$$
where

$$m^F = \left(\Delta T^F / \Delta q^F \right)^2$$
$$C_{jk} = B_{ik} B_{ij}$$

- The indices $i, j,$ and k take on values of nodes at which h is sought.

- Relating temperatures and heat fluxes established by re-casting the BEM equations as,

$$T_i^F = \bar{H}_{ik}^{FF} G_{kj}^{FF} q_j^F + d_i^F$$

where

$$\bar{H}_{ik}^{FF} = (\widehat{H}_{ik}^{FF})^{-1}$$
$$d_i^F = \bar{H}_{ik}^{FF} c_k^F$$

- From this expression, the sensitivity coefficients are identified as,

$$X_{ij} = \partial T_i^F / \partial q_j^F = \bar{H}_{ik}^{FF} G_{kj}^{FF}$$

- There results the linear equation for the fluxes at the convective nodes

$$\left(X_{ij} X_{ik} + m^F \beta \, C_{jk} \right) q_k^F = X_{ij} \left(\widehat{T}_i^F - d_i^F \right)$$

10

- For each q value, use Newton's cooling law : $h = q_s/(T_{wall} - T_{ref})$

- Method is general, will predict 2-D and 3-D effects, can be used with <u>transient</u> or <u>steady temperature</u> measurements to predict:

  1. constant in time h distribution.

  2. transient h distributions.

- For steady state temperature measurements:

  1. run transient solution to steady state w/ assumed initial condition

  2. replace transient H and G by steady state forms and set $d_i^F = 0$

3. Numerical Example: backward facing step model
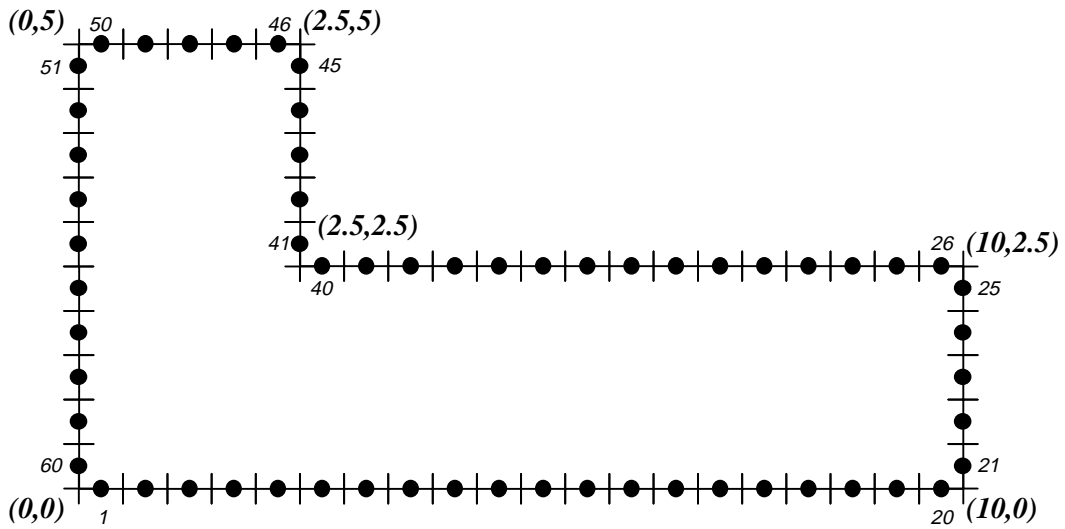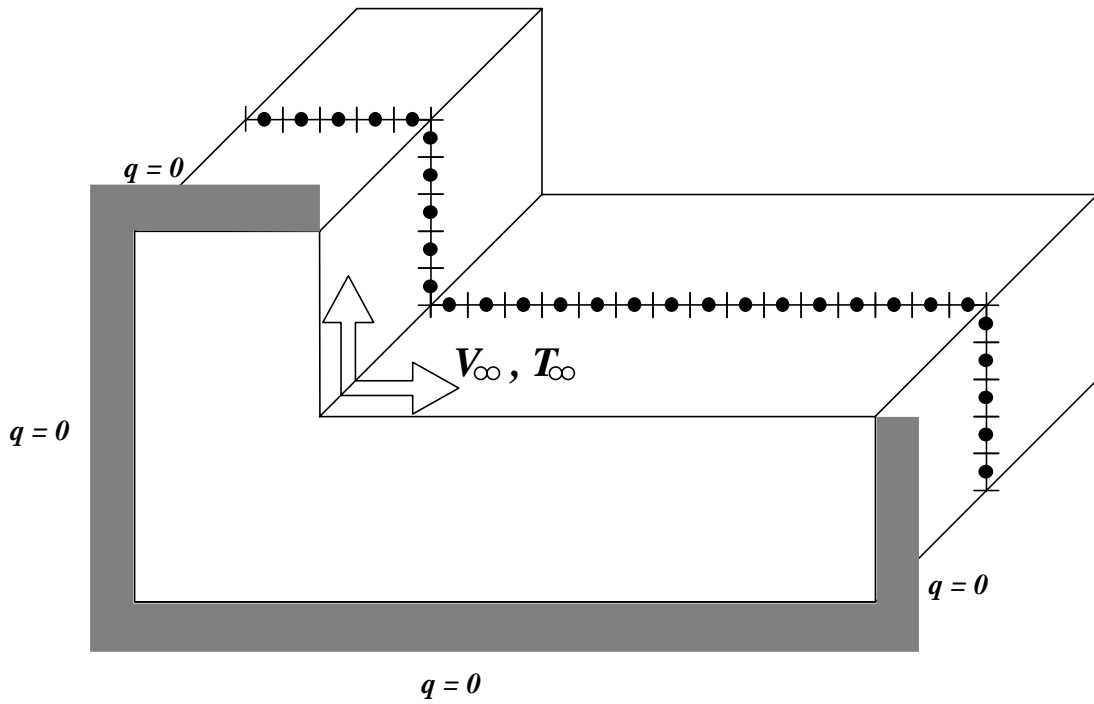
Figure 3.: BEM discretization for a backward facing step Aluminum: $k = 2.37W/cmK$, $\rho = 0.002702Kg/cm^3$, and $c = 903J/Kg$. $T_{ini} = 30°C$, $T_{amb} = 800°C$, $L = 5cm$, and h grows exponentially between $h = 0.01W/cm^2K$ at node 26 to $h = 0.074W/cm^2K$ at node 40, and decrease exponentially from $h = 0.055W/cm^2K$ at node 41 to $h = 0.0075W/cm^2K$ at node 45.
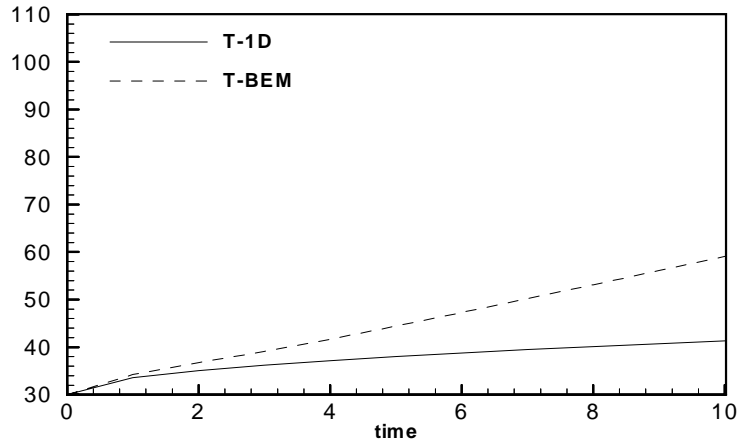
(a) node 26
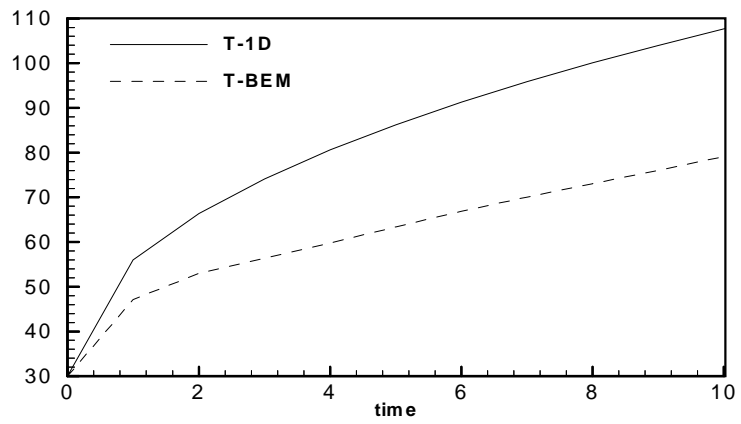
(b) node 40
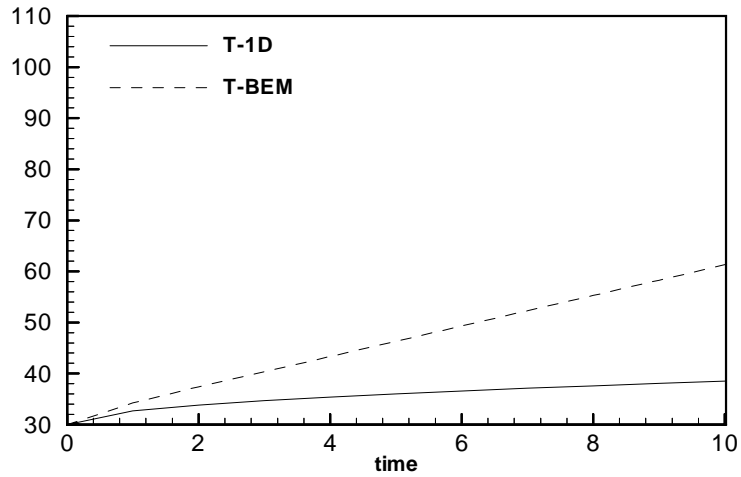
(c) node 45

Figure 4: Comparison of 1-D and BEM solutions

13
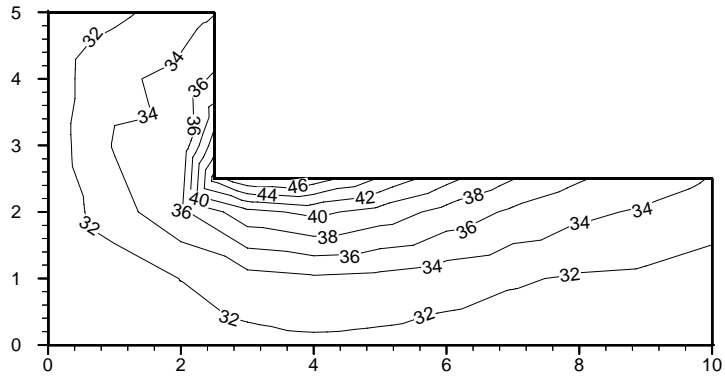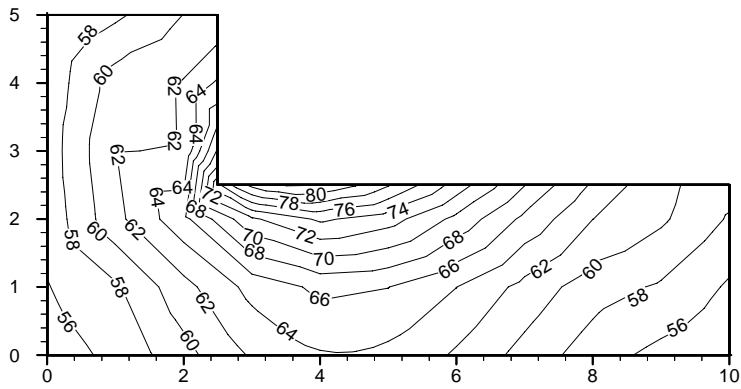
(a) after 1 second
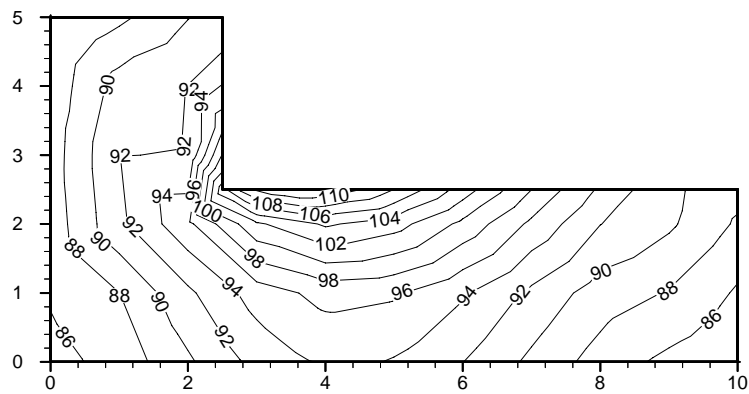
(b) after 10 seconds

(c) after 20 seconds

Figure 5: BEM retrieved isotherms
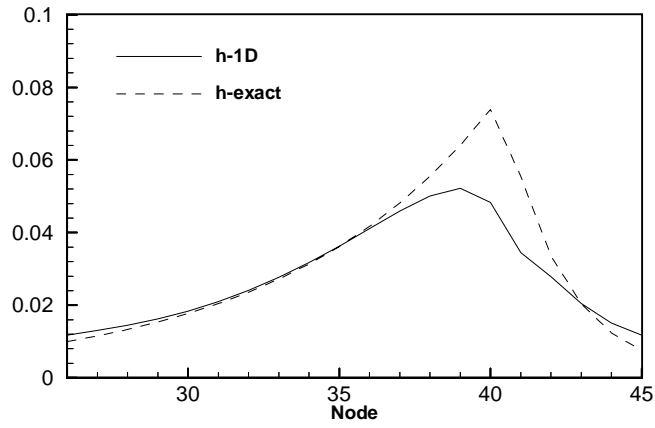
(a) after 1 second
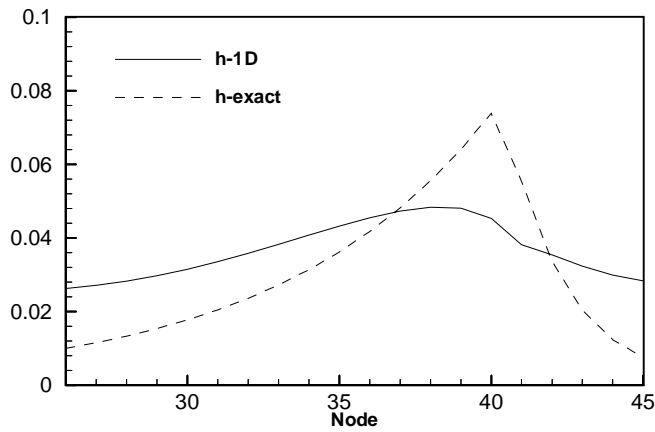
(b) after 10 seconds
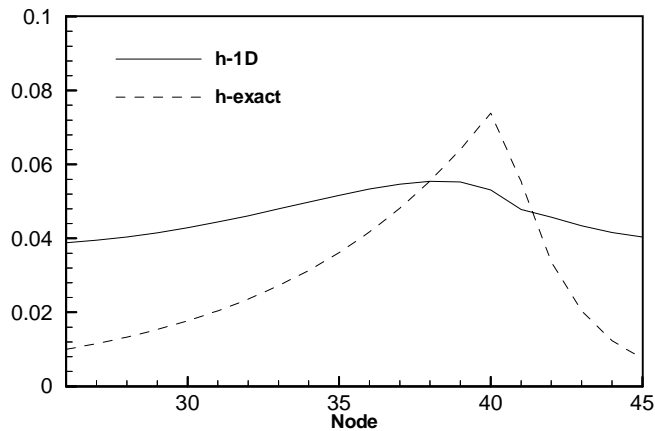
(c) after 20 seconds

Figure 6: Comparison of 1 D retrieved and exact film co-efficients
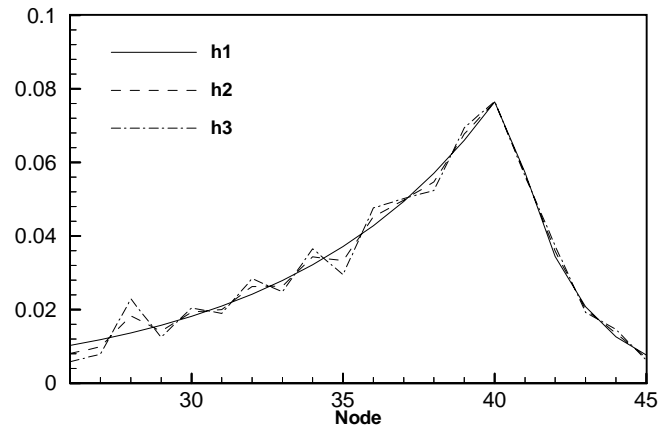
(a) after 1 second
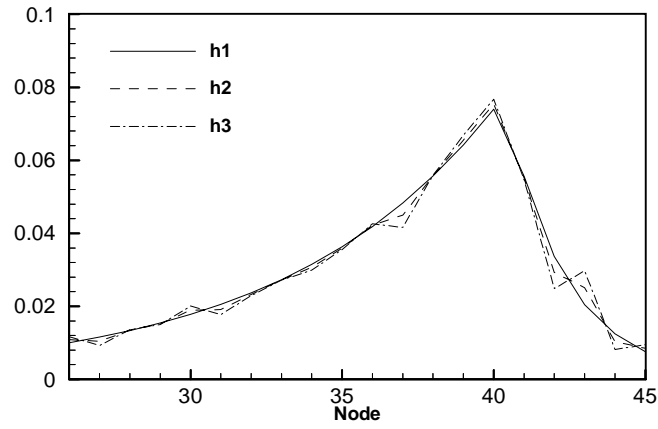
(b) after 10 seconds
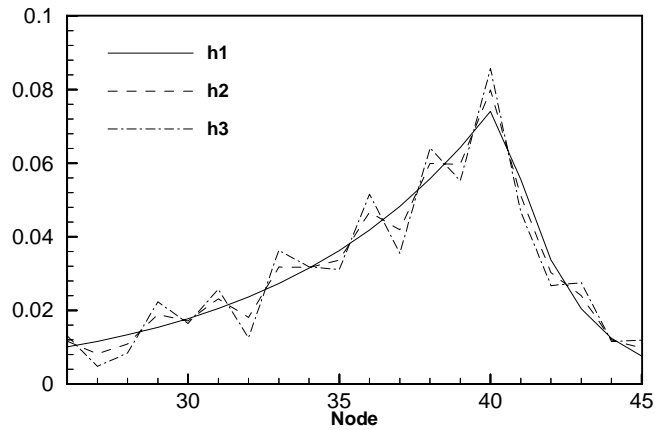
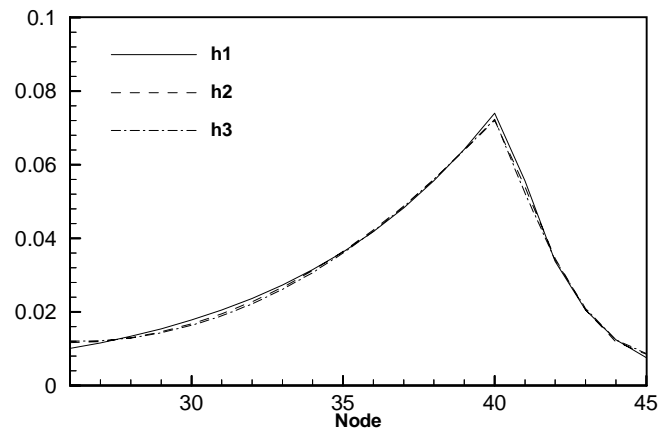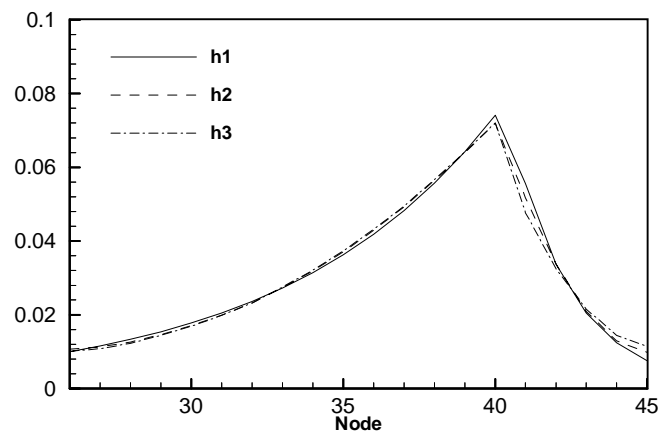(c) after 20 seconds

Figure 7: Comparison of BEM retrieved film coefficients with measurement errors: $\pm 0°$C for h1, $\pm 0.5°$C for h2, and $\pm 1°$C for h3. $\beta = 0$.

16
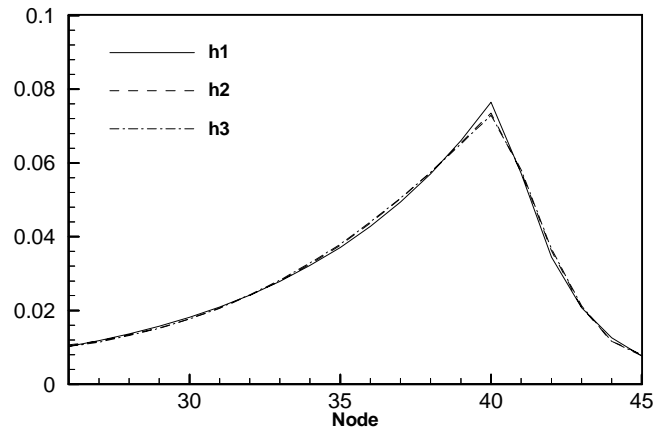
(a) after 1 second

(b) after 10 seconds

(c) after 20 seconds

Figure 8: Comparison of BEM retrieved film coefficients with measurement errors: $\pm 0°C$ for h1,$\pm 0.5°C$ for h2, and $\pm 1°C$ for h3 w/ $\beta = 5\sigma$.

17

D. Preliminary Results for Tip Heat Transfer Using Thermochromic Liquid Crystal

A schematic of the test set up is displayed in Figure 9. A blower supplies ambient air to the flow conditioning section. Upon exiting the blower, inlet air is heated from room temperature to 60°C via a heat exchanger. Water is supplied to the heat exchanger through an externally heated water supply and pump system that is computer controlled to maintain constant flow temperature based on a flow temperature measurement prior to the test section. The flow then passes through a flow conditioning section and is allowed to fully develop through a small section where a traversing Pitot tube is utilized to determine the flow rate.

The test section is shown in Figure 9 along with the BEM discretization used in the inverse analysis: 20 nodes on the front surface and 11 nodes on the top surface. In the experiment, air flows over a block of 2024 T-6 Aluminum coated with Thermochromic Liquid Crystal (TLC) on a black background, simulating a plane turbine blade tip surface. Properties of the block are: $k = 1.77 W/cmK$, $\rho = 0.00277 \ kg/cm^3, c = 875 \ J/kgK$. All other boundaries are constructed from acrylic plastic to allow viewing the test block from all directions. The flow is exhausted back to the ambient surroundings. The TLC coating is commercially available wide band micro-encapsulated chiral nematic thermochromic liquid crystal. The TLC is applied to two block surfaces using a high volume low-pressure gravity feed spray gun that applies a 0.1-0.2 mm thick coating. The TLC displays a color response to temperature via lattice re-orientation of the crystal. The temperature range that the TLC displays color is 35°C to 55°C, otherwise it is transparent to the background (black). The temperature entering the system is at the upper end of this range to allow the TLC the full range for response. The viewing system consists of a JVC 640x480 RGB CCD camera that is connected to a Pentium based PC for image processing and recording. A camera and a mirror arrangement are used such that one image contains two TLC-coated faces of the block with almost normal viewing. A computer program separates the sides and aligns pixels with position on the test block. In-situ pixel by pixel calibration is performed to account for viewing angle effects. The test block arrangement simulates a flat blade tip clearance gap in a turbomachine, and it is 178 mm in the cross-stream direction and 102 mm (L) in the stream wise direction from the simulated blade pressure (top) to suction side (right), see Fig. 9, where the BEM discretization and boundary conditions are also shown. An array of thermocouples provides temperatures at the left and bottom portions of the block. The simulated blade clearance gap is 5 mm (H) to give a stream wise length to clearance gap ratio of L/H=20.4. The Reynolds number, based on the hydraulic diameter, $D_H = 2H$, is Re_{D_H}=45x10^3. Two thermocouples and static pressure taps are included on the test block to verify temperature and alignment and to measure pressure drop. The first pressure tap and thermocouple are placed a distance of 3H upstream of the simulated blade tip, while the second pair are placed a distance of 10H downstream.

The block is first heated to a steady state temperature of $51°C$. Subsequently, flow is established within a fraction of a second by introducing inlet air initially at a temperature of $T_{in} = 48°C$ into the wind tunnel. The heater is turned off, and inlet air is allowed to cool. Inlet air reaches $30 \,°C$ over a period of $2\frac{1}{2}$ minutes after the heater is turned off, and remains at that temperature throughout the test. The inlet temperature is the reference temperature used in defining h. Images of both TLC-coated surfaces were taken at 31 second intervals and were processed as in calibration. Resultant hue values were converted to temperature at each time step using calibration curves for the point. These temperatures, as well as the thermocouple readings
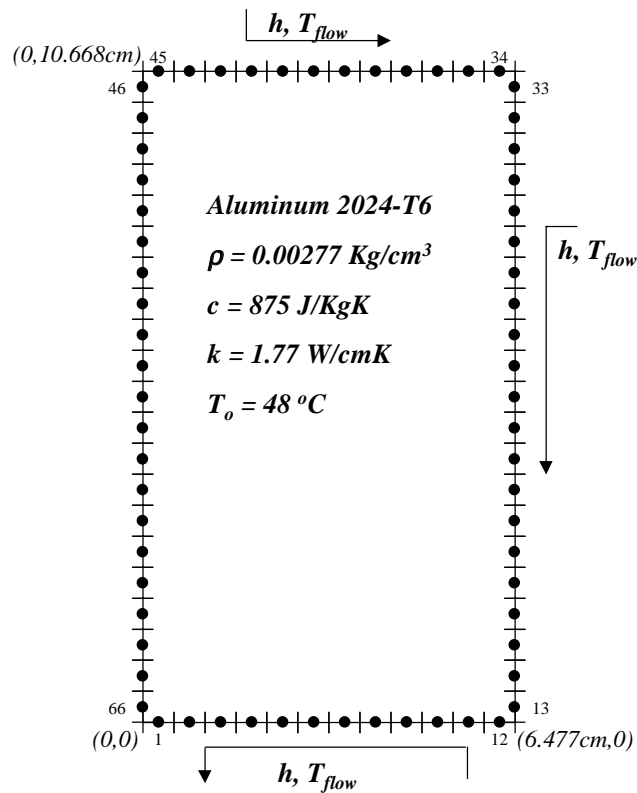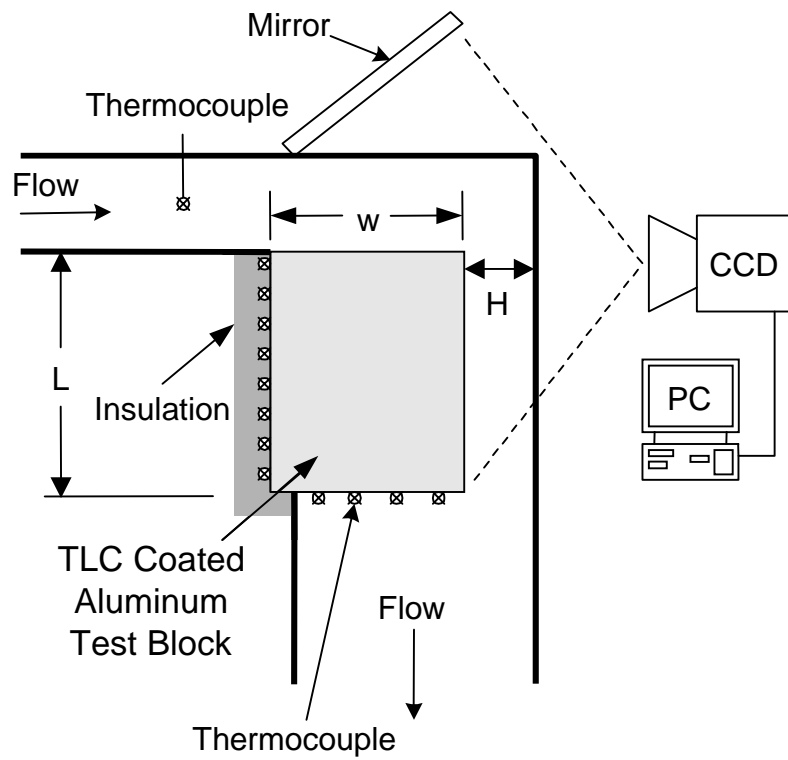
Mirror

Thermocouple

Flow

w

CCD

H

L

PC

Insulation

TLC Coated
Aluminum
Test Block

Flow

Thermocouple

h, T_{flow}

$(0,10.668cm)$ 45   34

46   33

h, T_{flow}

Aluminum 2024-T6

$\rho = 0.00277\ Kg/cm^3$

$c = 875\ J/KgK$

$k = 1.77\ W/cmK$

$T_o = 48\ ^oC$

66   13

$(0,0)$ 1   12 $(6.477cm,0)$

h, T_{flow}

Figure 9: TLC-coated test section arrangement, dimensions,
BEM- discretization and boundary conditions.
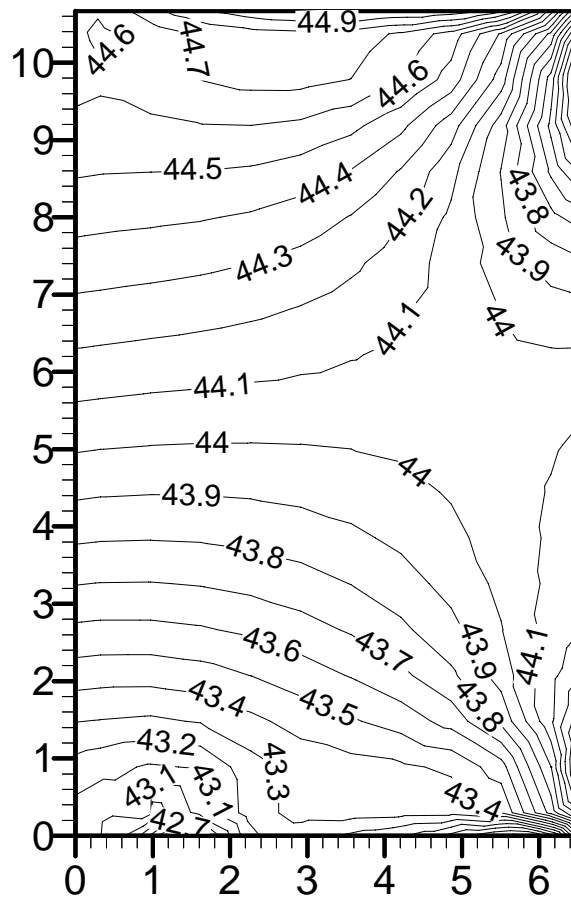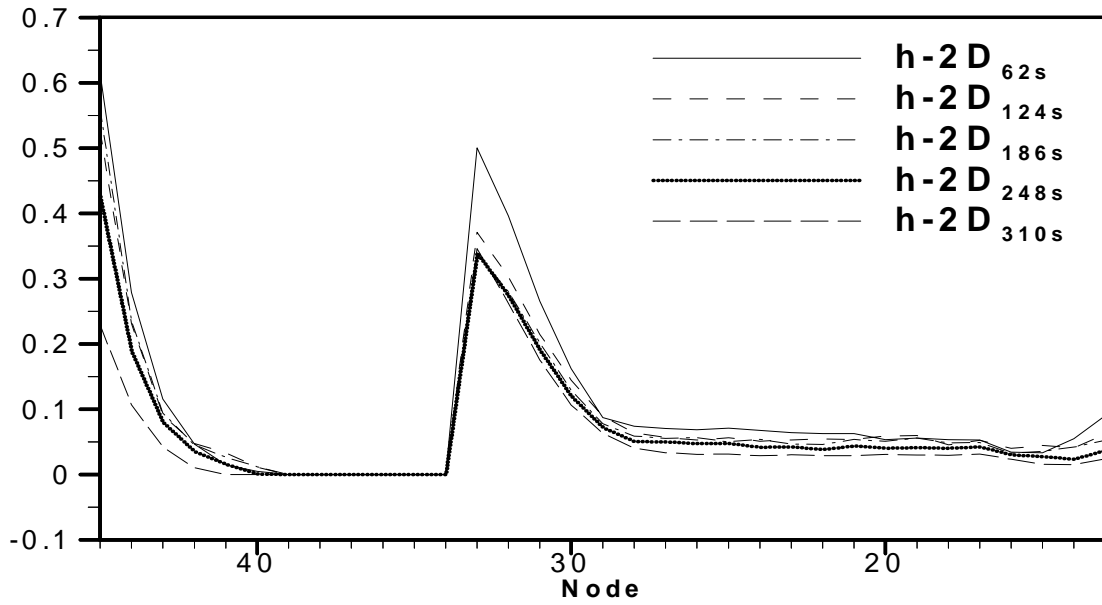
Figure 10: Distribution of heat transfer co-efficient at different time

were used as input to retrieve the h distribution over the test block. Retrieved h values are plotted in Fig. 10 for times $t = 62, 124, 186, 248$ and $310s$, along the top and right-hand-side surfaces, and an isotherm plot is provided in Fig. 10 for time t =186 s (h values are reported in W/cm^2K). As expected, h is seen to be relatively constant in time (certainly for times $> 62s$). The value of h decreases from 0.55 at the leading edge of the test section to nearly a value of zero at node 4, located nearly midway across the top surface. Examination of the isotherms reveals that due to the high heat transfer rate at the re-attachment point of the separated region (near node 32) on the front surface downstream of the corner, high rates of energy are drawn from the region downstream of the corner adjacent to node 32, thereby reducing heat loss from second half of the top surface upstream of the corner. Energy flows nearly parallel to the second half of the top surface towards the vicinity of node 32. As evidenced in the plot, h increases sharply as the flow goes around the corner and re-attaches at node 32. The nearly lateral heat transfer feature occurs in conducting materials such as the one used in this experiment and in practical applications. This would be undiscernible to the 1-D model. However, if the test block material were a poor conductor, then lateral heat transfer effects would be negligible. As expected, the value of h at re-attachement point, node 32, is nearly the same as at the leading edge of the top surface (node 45). Subsequently, the heat transfer rate decreases as we progress towards node 13 at the bottom of the front surface. Moreover, on the second half of the top surface h is nearly zero (and displayed as zero) and very sensitive to input error.
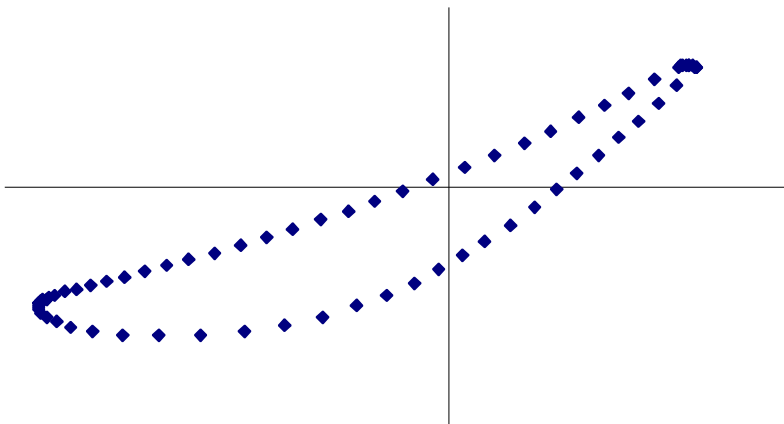
E. GE E³ Profiles

Pro/ENGINEER Models are currently being prepared. Plastic models to be used in casting will be fabricated from the Pro/E models by Rapid Prototyping.
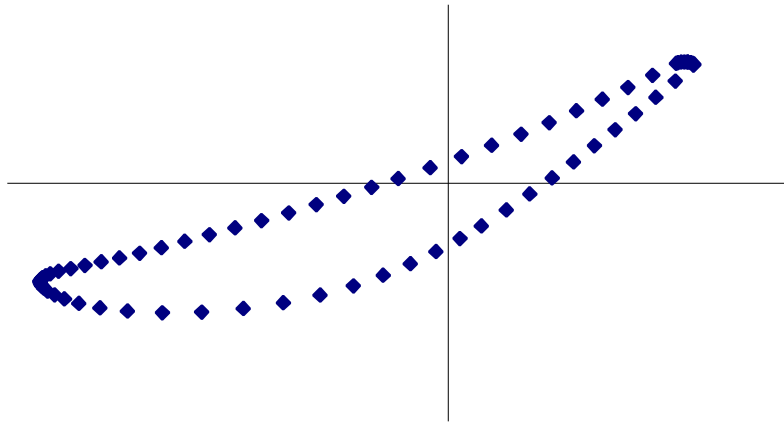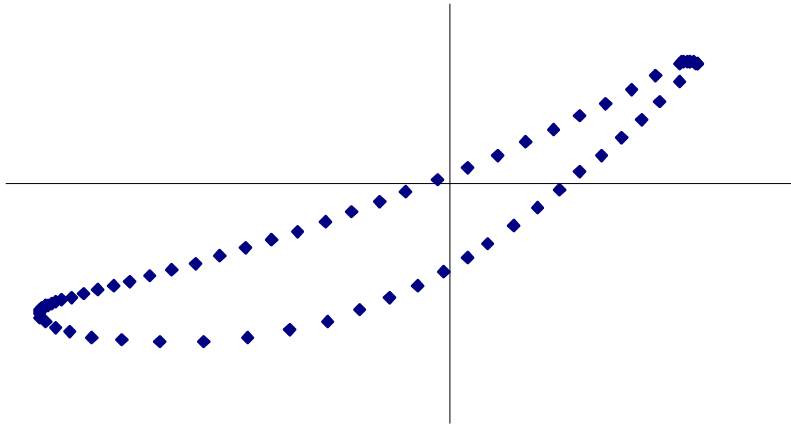

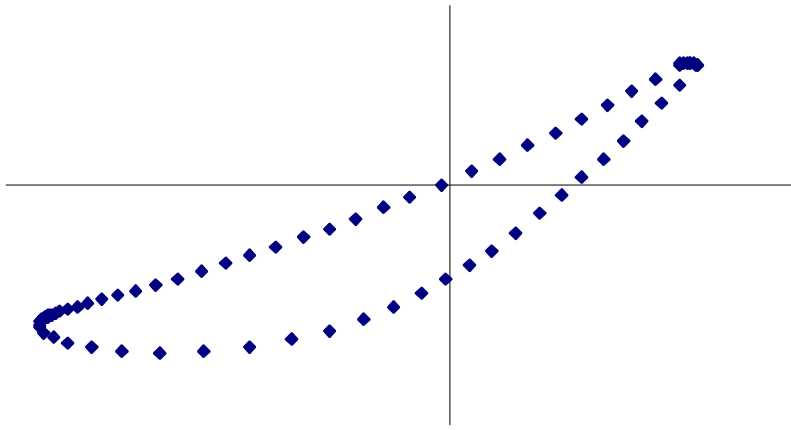(a) Rotor section A-A (hub)
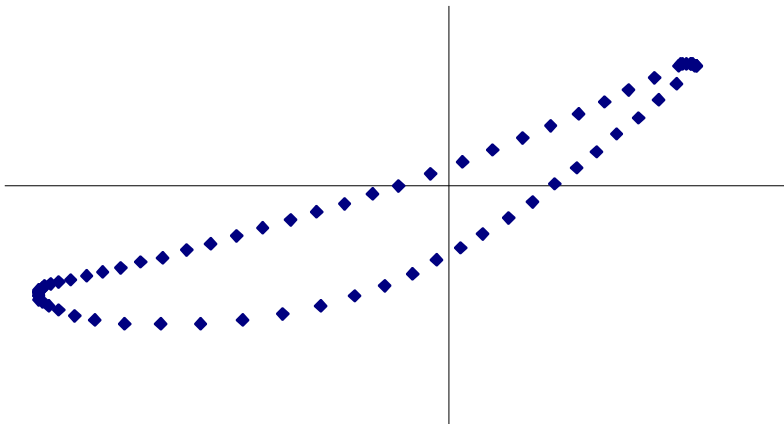
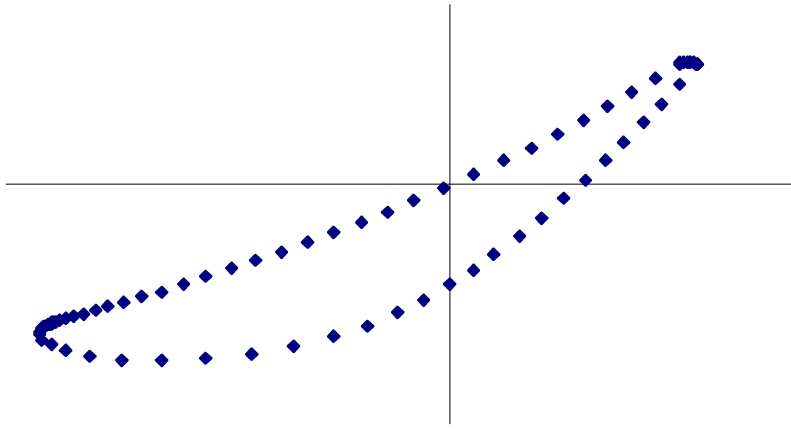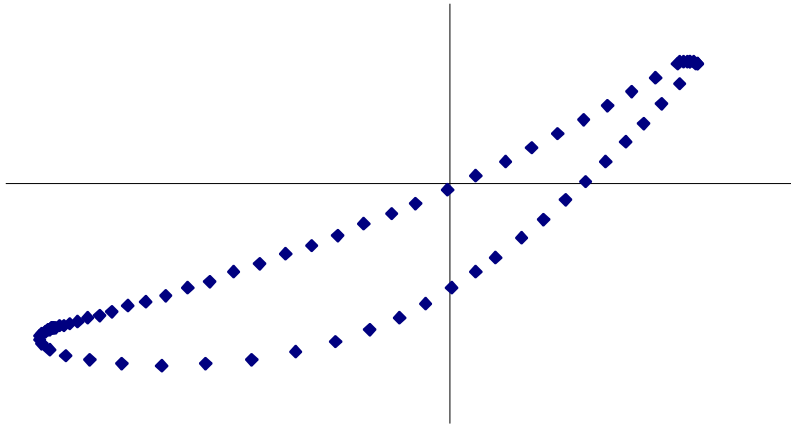(b) Rotor section B-B

(c) Rotor section C-C

(d) Rotor section D-D
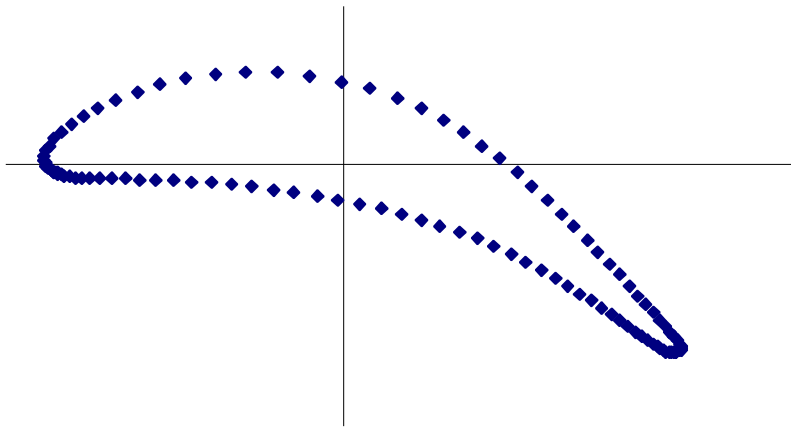

(e) Rotor section E-E
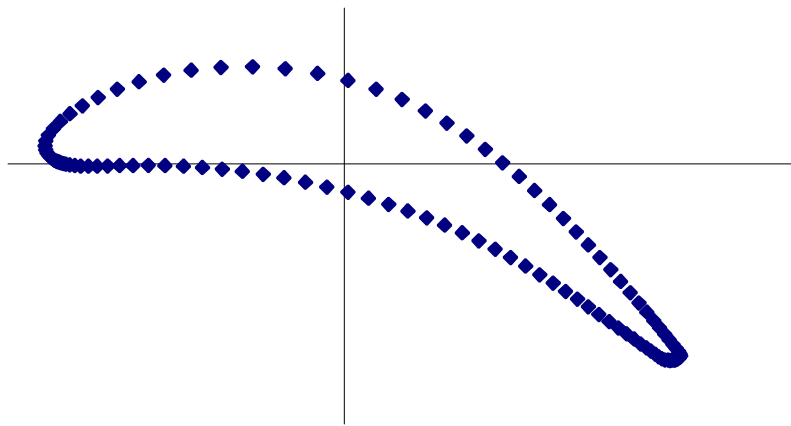
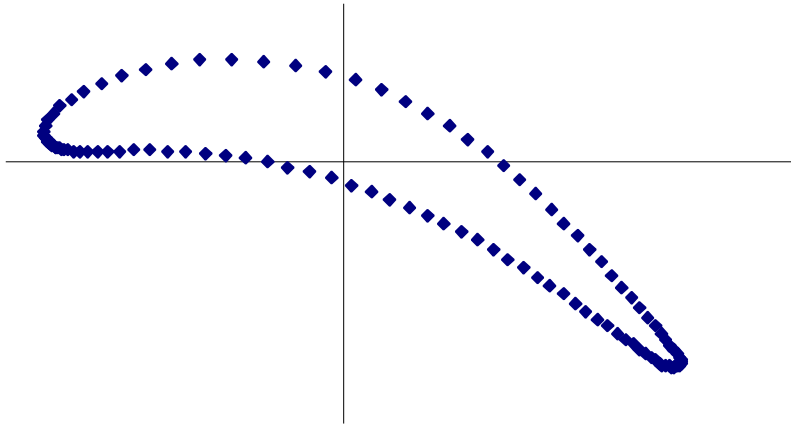

(f) Rotor section F-F

(g) Rotor section G-G (tip)
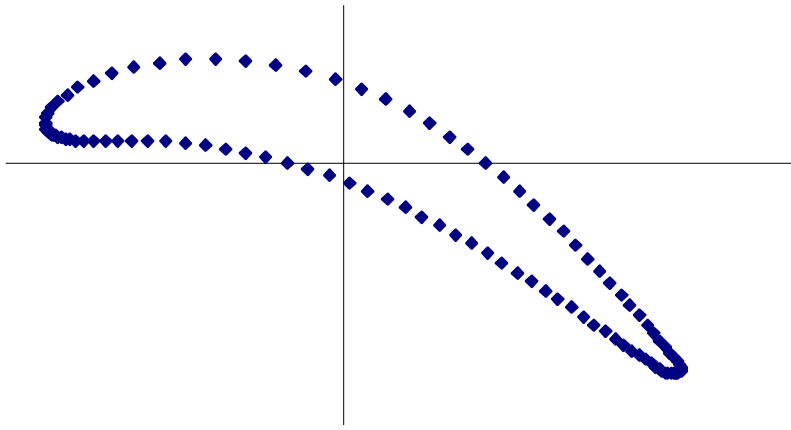
Figure 12: Rotor sections
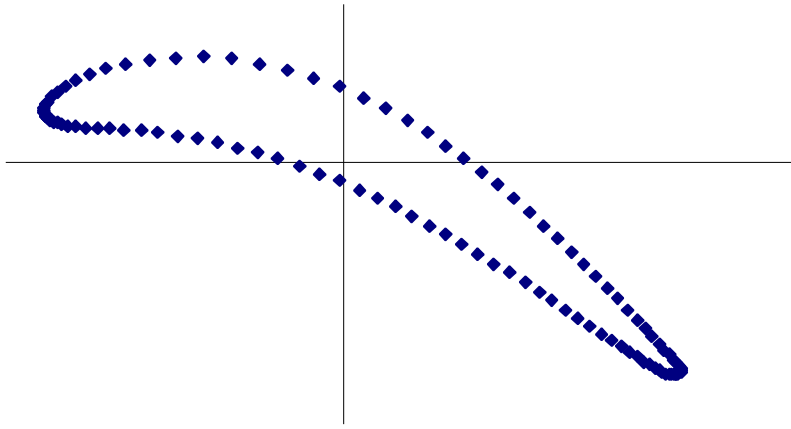

(a) Stator section A-A (hub)
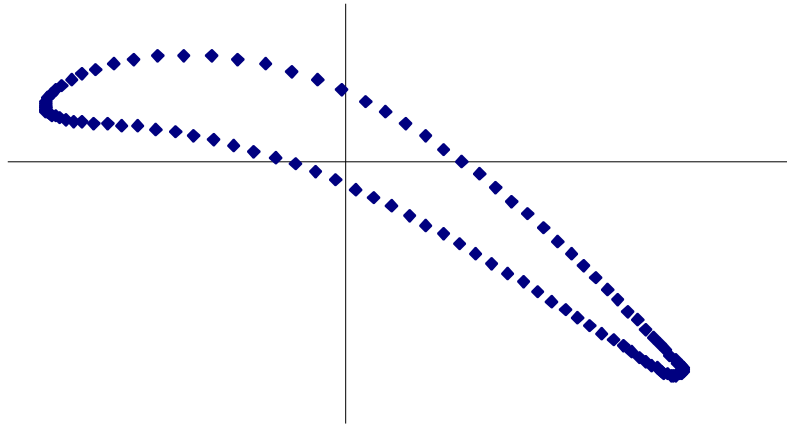

(b) Stator section B-B

(c) Stator section C-C

(d) Stator section D-D

(e) Stator section E-E

(f) Stator section F-F (tip)

Figure 13: Stator sections

F. Related Projects

NSF (CTS): Reconstruction of Multi-Dimensional Convective Heat Transfer Coefficient Distributions Using an Inverse BEM-Based Problem Approach.

NASA (GRC): Investigation of Conjugate Heat Transfer in Turbine Blades and Vanes.